THE ASTROPHYSICAL JOURNAL, 444:119–128, 1995 May 1

STAR FORMATION ACTIVITY IN SPIRAL GALAXY DISKS AND THE PROPERTIES OF RADIO HALOS: OBSERVATIONAL EVIDENCE FOR A DIRECT DEPENDENCE

MICHAEL DAHLEM
Space Telescope Science Institute, 3700 San Martin Drive, Baltimore, MD; dahlem@stsci.edu; and Johns Hopkins University, Department of Physics and Astronomy
UTE LISENFELD
Mullard Radio Astronomy Observatory, Cavendish Laboratory, Madingley Road, Cambridge CB3 0HE, England
AND
GÖTZ GOLLA
University of Toronto, Department of Astronomy, 60 St. George Street, Toronto, Ontario, Canada, M5S 1A7
Received 1994 June 6; accepted 1994 November 7

ABSTRACT

In this article we address observationally the questions: how does star formation (SF) in the disks of galaxies lead to the creation of radio halos, and what minimum energy input into the ISM is needed to facilitate this? For the investigation we use a sample of five edge-on galaxies exhibiting radio continuum emission in their halos and enhanced SF spread over large parts of their disks.

In a detailed study of the two galaxies in our sample for which we have the best data, NGC 891 and NGC 4631, we show that the radio halos cut off abruptly at galactocentric radii smaller than those of the underlying thin radio disks. Our most important result is that the halo cutoffs are spatially coincident with the radii where the SF activity in the underlying disks drops sharply. The difference in radius of the emission distributions tracing ongoing SF in the disks (*IRAS* 50 μm, Hα) versus that of the nonthermal radio continuum thin disks (tracing the distribution of cosmic-ray [CR] electrons) is typically a few kpc. This difference in extent is caused by CR diffusion. We have measured the CR diffusion coefficients in the thin disks of both NGC 891 and NGC 4631. For radial diffusion of CR electrons within the galactic disks the values are $D_r = 1.1$–2.5×10^{29} cm^2 s^{-1} (NGC 4631) and $D_r = 1.2 \times 10^{29}$ cm^2 s^{-1} (NGC 891). For motions in the z-direction in areas within the thin disks where no outflows occur, we derive a firm upper limit of $D_z \leq 0.2 \times 10^{28}$ cm^2 s^{-1} for NGC 891. The value for NGC 4631 is $D_z = 1.4 \times 10^{28}$ cm^2 s^{-1}.

The other three galaxies in our sample, NGC 3044, NGC 4666, and NGC 5775 show (at the sensitivity of our data) less extended, more filamentary radio halos. Isolated spurs or filaments of nonthermal radio continuum emission in their halos are traced only above the most actively star-forming regions in the disks. This, in conjunction with the results obtained for NGC 891 and NGC 4631, suggests a direct connection between the shapes and radial extents of radio halos of normal galaxies and the level and the spatial distribution of the current SF in their disks. The existence of filamentary structures implies that expansion and convection of CR-heated plasma plays an important role even at low z-distances above the plane.

Based on radio data we derive the disk-averaged mean energy input rates into the ISM due to supernova explosions per unit surface area in nine galaxies, including the ones in our sample. We find a clear trend in the sense that the galaxies with the highest mean energy input rates in the underlying disks have the most extended and pervasive radio halos. Below a certain threshold, outflows are inhibited. As a lower limit for this threshold we derive an energy input rate of $\sim 10^{-4}$ ergs s^{-1} cm^{-2}. The fact that radio halo emission is found only above the most luminous giant H II regions in late-type "normal" galaxies (of type Sbc or later) indicates that only these are capable of initiating disk-halo interactions by locally exceeding the threshold. The distribution of the local outflows determines the overall shapes of the CR halos and leads to the observed filamentary structures.

Subject headings: galaxies: individual (NGC 891, NGC 4631) — galaxies: spiral — radio continuum: galaxies — stars: formation

1. INTRODUCTION

Field, Goldsmith, & Habing (1969) presented a two-phase model of the Galactic interstellar medium (ISM), in which they describe the stability of two phases in pressure equilibrium, namely, cold gas at $T_c \simeq 30$ K and a density of $n_c \sim 100$ cm^{-3}, and a warm component with $T_w \sim 8 \times 10^3$ K and $n_w \sim 0.4$ cm^{-3}.

Later observations, particularly in the extreme ultraviolet (EUV) and the soft X-ray regime, pointed at the existence of a third, hot component of the ISM, with a temperature in the range of $T_h \sim 10^6$ K and $n_h \sim 0.01$ cm^{-3}. A three-phase model of the ISM accounting for the third component has been made by McKee & Ostriker (1977).

The increasing sensitivity of receivers and angular resolving power subsequently made it possible to compare the ISM in the Milky Way with that of nearby external galaxies and has yielded an overview of the star formation (SF) properties of these galaxies. The local composition of the ISM in external

galaxies, as well as our own, depends on the star formation rate (SFR), and the two- and three-phase models may be considered as the most extreme cases in this scenario. The two-phase model describes quiescent galaxy disks (or parts thereof), while the three-phase mode—with the dominant hot ionized component—is a fairly good description of areas with ongoing massive SF. It was recognized, e.g., by Habe & Ikeuchi (1981), that massive SF can lead to outflows of matter from galaxy disks (see also Tomisaka, Ikeuchi, & Habe 1981) and that in this case exchanges of gas between disks and halos are not negligible.

Subsequent models of the ISM included an exchange of matter between galaxy disks and the surrounding halos. The best known are the "galactic fountain" model by Shapiro & Field (1976) and the "chimney" model by Ikeuchi (1988) and Norman & Ikeuchi (1989, hereafter NI). In addition to the exchange of gas, cosmic rays (CRs) and magnetic fields may also take part in disk-halo interactions, leading to the formation of radio halos around galaxies (cf. Parker 1992 and references therein).

In this paper we want to address observationally the question of how SF in the disks of galaxies can lead to the creation of radio halos and in particular, what minimum energy input into the ISM is needed to facilitate this. For studies of halos of spiral galaxies, maps of edge-on systems are particularly well suited. We will consider only spirals with enhanced SF spread over large parts of their disks; nuclear starbursts will be excluded from the present study. This selection has been quantified by Lehnert & Heckman (1995), based on the optical half-light radii in the broad-band (R-filter) and in Hα. "Normal" disk galaxies with enhanced SF have $\log (R_{H\alpha}/R_R) \simeq 0$, while $\log (R_{H\alpha}/R_R) \simeq -0.6$ for nuclear starbursts.

Measurements of the disk emissivity are available for a considerable number of edge-on galaxies, but only a few percent of the—optically selected edge-on—galaxies studied by Hummel, Beck, & Dettmar (1991b) show signs of radio halos. Together with the previously known cases, and after exclusion of nuclear starburst galaxies, presently only five late-type spirals with radio continuum emission from their halos are known. All of them are viewed at very high inclination angles, $i \geq 75°$; they are NGC 891, NGC 3044, NGC 4631, NGC 4666, and NGC 5775.

NGC 891, NGC 4631, and NGC 5775 are the three galaxies with the most extended radio halos. All three show ongoing SF over large fractions of their disks.

NGC 4631 was the first galaxy in which a radio halo was detected (Ekers & Sancisi 1977). More recent observations at 1.5 GHz were published by Hummel et al. (1988). Their total intensity map is reproduced in Figure 1. It indicates the existence of an extended halo of radio emission in which a prominent radio continuum spur can be seen, the nature of which is discussed in more detail by Golla & Hummel (1994).

The second radio halo was found by Allen, Baldwin, & Sancisi (1978) in NGC 891. Data with higher sensitivity were obtained by Hummel et al. (1991c; their Fig. 2). This map is displayed in Figure 2. In both NGC 891 and NGC 4631, Hummel et al. (1991c) conducted spectral index investigations which suggested the presence of large-scale galactic winds. Currently, the most sensitive and highest resolution radio continuum map of an edge-on galaxy is that of NGC 891 by

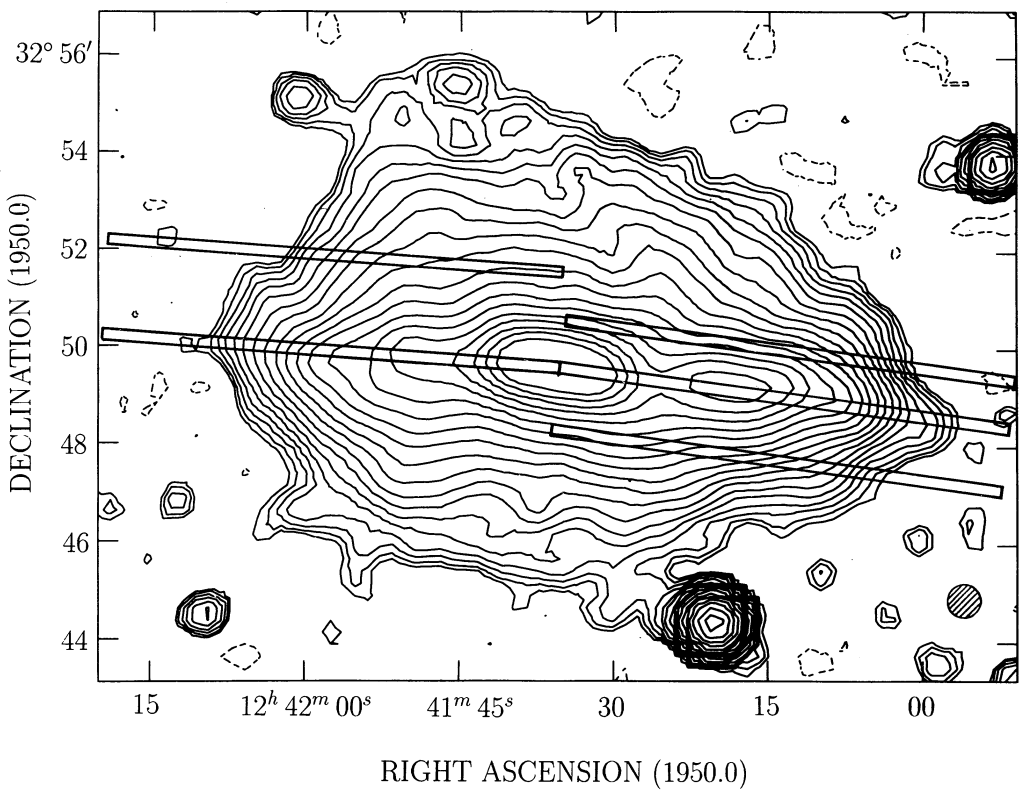

FIG. 1.—1.49 GHz radio map of NGC 4631 by Hummel et al. (1988) with a resolution (HPBW) of 40″. The contour levels are −0.1, 0.1, (2.5 σ), 0.14, 0.2, 0.28, ..., 51.2 mJy beam^{-1} in $2^{N/2}$ spacings.

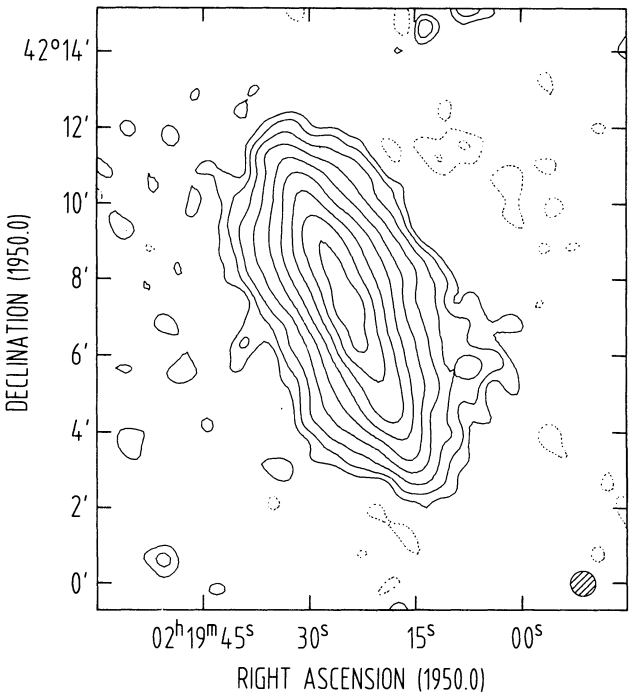

FIG. 2.—1.49 GHz VLA D array map of NGC 891 (Hummel et al. 1991c) with a resolution of 40″. The contours show flux densities of −0.4, −0.2, 0.2 (2.5 σ), 0.4, 0.8, ..., 51.2 mJy beam^{-1}.

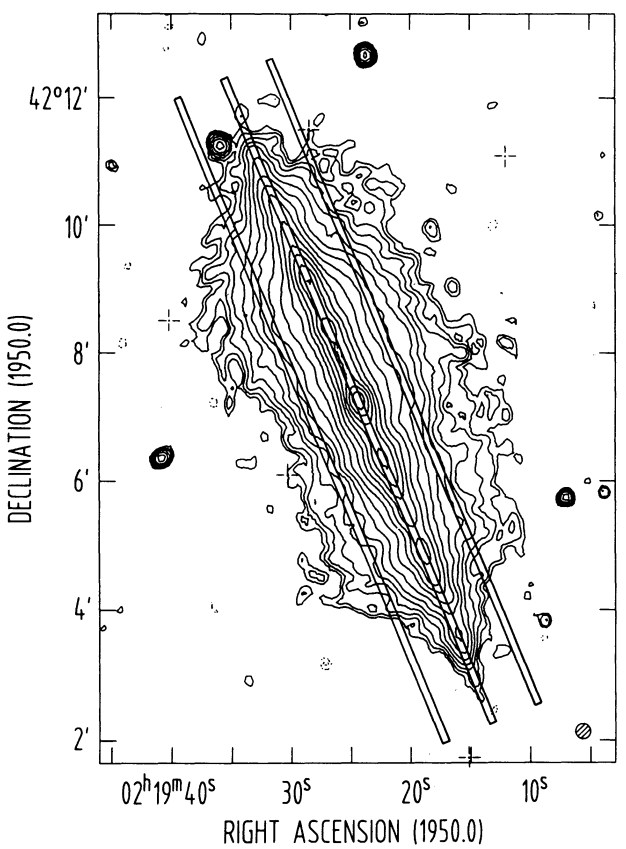

FIG. 3.—1.49 GHz map of NGC 891 of the VLA C+D array by Dahlem et al. (1994) with a resolution of 13″ (600 pc). The contour levels are −0.12, 0.12 (3 σ), 0.17, 0.24, 0.34, ..., 21.7 mJy beam^{-1}.

Dahlem, Dettmar, & Hummel (1994), which was obtained with the VLA[1] (Fig. 3). Here, the thin disk and halo emission can be separated very clearly. For NGC 891 and NGC 4631, a detailed analysis of their SF properties and their radio halos has been carried out (§ 2).

The first radio map of NGC 5775 showing out-of-the-plane emission was published by Duric & Bloemen (1989). Dettmar & Golla (1995) obtained more sensitive data exhibiting the presence of several radio continuum filaments which are associated with the most conspicuous Hα filaments in the halo. A new very deep map of NGC 5775 by Irwin (1994) shows the presence of an extended diffuse radio halo with a z-extent of the order of 10 kpc. Unfortunately, the data of NGC 5775 by Dettmar & Golla (1994), which we use for the present study, are not sensitive enough for detailed measurements as carried out for NGC 891 and NGC 4631. Thus, only global SF properties like, e.g., the energy input rate by supernovae (SNs) and supernova remnants (SNRs) into the ISM, can be derived. The same holds for the two remaining galaxies with high-z radio emission, NGC 3044 and NGC 4666 (§§ 3 and 5).

Hummel & van der Hulst (1989) show a 1.49 GHz map of NGC 3044 (their Plate 3), with weak halo emission above the thin disk in a relatively small radial regime north of the nucleus, extending by about 20″ toward east. J. A. Irwin (1994, private communication) also reports high-latitude radio continuum in NGC 3044.

Sukumar, Velusamy, & Klein (1988) obtained a 4.9 GHz map of NGC 4666 with the VLA (their Plate 3), which also exhibits radio continuum emission from its halo.

These five galaxies will be compared with other, edge-on late-type, spirals which only have radio halos with lower z-extents—and with galaxies which do not exhibit radio emission from outside their thin disks (§ 5). Additional calculations of energy densities and CR diffusion coefficients in NGC 891 and NGC 4631 will be presented in §§ 5.3 and 6. § 7 gives a summary.

2. SPATIAL EMISSION DISTRIBUTIONS IN THE DISKS AND HALOS OF NGC 891 AND NGC 4631

CR electrons, as well as associated protons, are commonly thought to be produced by SNs of Types Ib and II. Thus, it is reasonable to adopt as the distribution of CR-emitting sources the locations of SF regions in galaxy disks.[2] In order to determine whether there is a direct relation between the current SF in galaxy disks, subsequent SN events, and the properties of their halos, we must quantitatively measure and compare the morphologies of both the disk and halo emission components.

For this purpose, we use maps of edge-on galaxies to compare the *radial extents* of the thin disks with those of their radio halos. Within the thin disks we measure the radial extent of the synchrotron emission as well as the radius of that part of the disk where SF is currently occurring at a high level. The best observable tracers of SF activity in galaxies are Hα recombination radiation, FIR dust emission, and thermal radio continuum from H II regions. The term "radial distances" will be

[1] The VLA is a facility of the National Radio Astronomy Observatory, which is operated by Associated Universities, Inc., under contract with the National Science Foundation.

[2] When talking about cosmic rays (CRs), we will actually be referring to CR electrons, because nonthermal radio continuum emission of relativistic electrons is the only measurable radiation process tracing CRs in external galaxies.

TABLE 1

RADII OF CR HALOS AND COMPARISON WITH THIN NONTHERMAL RADIO DISKS AND 50 μm FIR/Hα EMISSION

OBJECT (1)	D (Mpc) (2)	r_{CR} (arcmin) (3)	r_{CR} (kpc) (4)	r_{halo} (arcmin) (5)	r_{halo} (kpc) (6)	r_{SF} (arcmin) (7)	r_{SF} (kpc) (8)	Δr (kpc) (9)	B_{disk} (μG) (10)	t_e (10^7 yr) (11)	D_r (10^{29} cm^2 s^{-1}) (12)
NGC 891	9.5	4.63 (13″)	12.8	3.38 (13″)	9.4	3.33[a] (80″)	9.6	3.2 ± 0.6	10[b]	2.5	1.2
NGC 4631 W.....	10.0	8.20	23.8	7.01	20.4	6.03	17.6	6.2 ± 1.0	6.5[b]	4.8	2.5
NGC 4631 E		7.21 (40″)	21.0	5.63 (40″)	16.4	5.80 (6″)	16.9	4.1 ± 1.0			1.1

[a] van Driel et al. 1993.
[b] Hummel et al. 1991c.

used in order to describe projected distances from the galaxy center along and parallel to the major axis.

In order to measure the radial extents of emission distributions we define a significance level or absolute flux density to which this is done; here, we choose to measure to the 2.5 σ significance level of the data. This biases our investigations with the sensitivity of the maps. However, due to the inhomogeneity of the datasets which we use, this is the only practical measuring technique.

2.1. *The Radial Extent of the Actively Star-forming Thin Disks*

For these investigations we use *IRAS* CPC and Hα images which are available to us.

NGC 891 is the only galaxy presented here for which a relatively good *IRAS* CPC 50 μm map (van Driel et al. 1993) is available, although it is affected by gain variations of the CPC detector which show up as stripes in the scanning direction. To measure the radial extent of the current star-forming disk, r_{SF}, we obtained a cut through the thin disk along the major axis and we find, at the 2.5 σ level, $r_{SF} = 9.2 \pm 0.8$ kpc[3]. Within the measuring accuracy, the same value has been derived by Dettmar (1990) from an Hα image. He notes that the southern cutoff is located symmetrically with respect to the one north of the center, at $r_{SF} = 10.0$ kpc. The median value derived on both sides of the center, from both datasets, $r_{SF} = 9.6$ kpc, is given in Table 1, columns (7) and (8).

Since the size of the maps obtained with the *IRAS* CPC detector is too small for imaging the entire disk of NGC 4631, an Hα image by Golla (1993) is used.

Because of the importance of the measuring techniques, we provide the basic parameters of the strip integrations separately in Table 2. The extents of the actively star-forming disks of NGC 891 and NGC 4631 can be measured with uncertainties in the range of 0.4–0.8 kpc.

One important quantity which follows directly from the measurements of r_{SF} is the surface area of those parts of the galaxy disks in which at present SF is occurring at a high level, $A_{SF} = 2\pi r_{SF}^2$. This surface area is only about one-half to two-thirds of the optically visible disks.

2.2. *The Thin Nonthermal Radio Continuum Disks*

For the derivation of the radii of the CR-emitting thin disks, r_{CR}, we use the best available radio continuum maps at 1.5 GHz of NGC 891 and NGC 4631. The former is shown in Figure 3 (from Dahlem et al. 1994). The r_{CR} is again measured at the 2.5 σ level (central cut). Beam-smearing is almost negligible at this resolution; the measuring accuracy is ±0.25 kpc.

The results for NGC 4631 (Fig. 1) have relative uncertainties of ±0.7 kpc. The relatively wide error margin is caused by the low resolution of this map of about 1.85 kpc. Note that the eastern half of NGC 4631 is tidally disturbed, which makes an interpretation of our data more uncertain than to the west of the center.

Comparing the numbers for r_{SF} and r_{CR} for both galaxies which are compiled in Table 1, it is clear at first sight that the nonthermal radio continuum emission of CRs in the thin disks extends radially further out than the tracers of SF, like FIR or Hα emission: $r_{CR} > r_{SF}$. The differences, $\Delta r = r_{CR} - r_{SF}$, are of the order of a few kpc (col. [9]). The uncertainty of $\Delta r = r_{CR} - r_{SF}$ is typically of the order of 0.6–1.0 kpc, i.e., in the range from 15% to 25% of the measured value.

2.3. *The Radial Extent of the Synchrotron Radio Halos*

For a quantitative comparison with r_{CR}, we also measured the radial extent of the CR radio halos, r_{halo}, for both NGC 891

[3] Throughout this paper we use distances derived by Tully (1988), which are based on $H_0 = 75$ km s^{-1} Mpc^{-1} and corrected for the Virgocentric flow; see Table 3, col. (3).

TABLE 2

PARAMETERS FOR CUTS

OBJECT	BAND	LOCATION (Disk/Halo)	HPBW	WIDTH	z-DISTANCE (HPBW)	z-DISTANCE (kpc)
NGC 891	1.49 GHz	Disk	13″	5″	0	0
	1.49 GHz	Halo	13	5	3.5	2.1
	50 μm	Disk	80	20	0	0
NGC 4631.....	1.49 GHz	Disk	40	15	0	0
	1.49 GHz	Halo	40	15	1.5/1.9	2.8/3.5
	Hα	Disk	6	15	0	0

and NGC 4631. These values come from two cuts each parallel to the major axes of both galaxies (cf. Figs. 1 and 3). Both the lengths and widths of the marked areas are to scale. This procedure is adapted to the resolution of the maps. In order to avoid contamination from the thin disks, the cuts are placed at different z-offsets, depending on the intrinsic thickness of the thin disks and on the resolution of the maps used (Table 2).

For the calculation of $r_{\rm halo}$, the values from both strips in the halos were averaged. The resulting values are given in Table 1, columns (5) and (6). The uncertainties of $r_{\rm halo}$ are in the range ± 0.3–0.7 kpc. Due to the above-mentioned disturbance in the eastern half of its disk, we could measure the halo extent of NGC 4631 only on one side, north of the disk. The difference in spatial resolution of the 1.5 GHz radio maps does not affect our results significantly, because $r_{\rm halo}$ varies only slowly as a function of z (see Fig. 3). We verified this by calculating $r_{\rm halo}$ from the low-resolution map of NGC 891 (Fig. 2), which yielded—within the error margins—the same results as for the high-resolution map.

2.4. *Comparison of Star-forming Disk and Halo: Spatially Correlated Radial Cutoffs*

From these measurements of $r_{\rm SF}$, $r_{\rm CR}$, and $r_{\rm halo}$, we can directly calculate the differences in radial extent of the actively star-forming parts of the disks, the thin nonthermal radio disks, and the halos. The $r_{\rm SF}$ and $r_{\rm halo}$ show a very good correspondence for both galaxies NGC 891 and NGC 4631. The values for the differences in radial extent of the radio continuum emission distributions, $r_{\rm CR} - r_{\rm halo}$, are more accurate than those for $\Delta r = r_{\rm CR} - r_{\rm SF}$ (§ 2.2), because for the former comparison both radii are measured in the same map for each galaxy. Hence, within the measuring accuracy, the radial extents of the star-forming disks and the radio halos are equal: $r_{\rm halo} \simeq r_{\rm SF}$, and thus $\Delta r = r_{\rm CR} - r_{\rm SF} \simeq r_{\rm CR} - r_{\rm halo}$ (see Table 1).

Dahlem et al. (1994) were the first to point out that the radial cutoff of the halo emission in NGC 891 occurs at the same galactocentric radius as that at which the SF activity in the thin galaxy disk drops rapidly. As tracers of the SF activity they used radial profiles of the 50 μm far-infrared (FIR) and Hα emission along the major axis of NGC 891. We have now quantified this and demonstrated the presence of the same effect in NGC 4631.

3. FILAMENTARY RADIO HALO EMISSION

The derivation of halo parameters like $r_{\rm halo}$ makes sense only for extended, pervasive halos, as observed in NGC 891 and NGC 4631. The high-sensitivity data by Irwin (1994) show that NGC 5775 also has an extended radio halo. Our data, however, only show the most prominent radio filaments due to lower sensitivity (Dettmar & Golla 1995). The radio halo emission in NGC 3044 is also less extended than in the above galaxies (Hummel & van der Hulst 1989). For NGC 4666 no firm statement can be made yet. Therefore, we will not attempt here to derive quantitative parameters of the halo emission distribution in these systems. The more filamentary (and/or lower surface brightness) emission seen there requires more detailed analyses of disk and halo emission with high angular resolution, which—based on the currently available data—are still very difficult to conduct.

Still, it should be realized (see citations in §§ 1 and 4) that the radio (and Hα) filaments in the halos of these galaxies follow the same rules as the emission distribution in extended halos: they are observed only above those parts of the thin disks where the most prominent SF regions are found. This suggests that the observed shapes of galactic radio halos depend on the number of radio continuum filaments and thereby on the number (or surface density) of the H II regions in the underlying thin disks. Evidence for this hypothesis has been found by Golla & Hummel (1994) in the form of a correlation between a prominent radio spur and an underlying giant H II region in NGC 4631 and their finding that the radio halo of NGC 4631 can be explained as a superposition of spurs or filaments connected with the activity in the underlying disk. Radio halos which—when observed with the same high sensitivity as NGC 891 and NGC 4631—are filamentary, would then suggest a lower mean surface density of SF regions in the disk.

4. SPATIAL CORRELATION OF EXTRAPLANAR Hα, X-RAY, AND RADIO HALO EMISSION

Hα observations of extraplanar ionized gas independently confirm the correlation of disk-halo interactions and underlying SF. In all the galaxies discussed here the radio halo emission is associated with diffuse ionized gaseous halos or filaments seen in Hα emission (for a review, see Dettmar 1992). In NGC 891, diffuse extraplanar Hα emission has been found only inside the radial boundaries of the radio halo, i.e., at $r \leq r_{\rm halo} \simeq r_{\rm SF}$ (Dahlem et al. 1994). In NGC 5775, Hα filaments are seen in association with radio continuum spurs (Dettmar & Golla 1995). In NGC 4631, the vertical scale height of the Hα emission is increased above the central region, where the SF activity is enhanced. The Hα emission from the halos of all five galaxies introduced in § 1 shows filamentary structure. The appropriate Hα images can be found in Dettmar (1990) and Rand, Kulkarni, & Hester (1990) for NGC 891; Rand, Kulkarni, & Hester (1992) for NGC 4631; Dettmar & Golla (1995) for NGC 5775; and Lehnert (1992) for NGC 4666 and NGC 3044.

In both NGC 4631 and NGC 891 (Wang et al. 1995; Bregman & Pildis 1994), diffuse soft X-ray emission was detected in their halos. No halo emission is seen at $r > r_{\rm SF}$. Thus, not only do the CR halos cut off abruptly at certain distances out from the center, but other components of the halo gas, i.e., 10^4 K and 10^6 K gas, respectively, do as well. In NGC 891, CO (García-Burillo et al. 1992) and H I gas (R. Swaters & J. M. van der Hulst 1994; private communication) have also been detected above the thin disk. This suggests that, once outflows occur, all components of the ISM are dragged out into the halo. The detection of polarized emission in the halos of NGC 891 and NGC 4631 (Hummel et al. 1988; Hummel, Beck, & Dahlem 1991a; Golla & Hummel 1994) indicates that this also includes ordered magnetic fields.

All these observations, together with the detection of filamentary radio emission above the most actively star-forming regions, illustrate the importance of expansive motions and convection, even at low z, as the process driving the outflows (cf. Dahlem et al. 1994; Golla & Hummel 1994). At high z there is observational evidence for convection in the form of large-scale galactic winds (e.g., Hummel et al. 1991c). Such winds have been modeled by Breitschwerdt, McKenzie, & Völk (1991, 1993). Other models, e.g., by Siemienec & Cesarsky (1991), show that diffusion can also play an important role, even at high distances above the planes. Purely diffusive CR propagation, however, cannot explain the filamentary features and the abrupt radial cutoffs of the halos.

5. THE ENERGY INPUT OF STAR FORMATION REGIONS INTO THE AMBIENT ISM

5.1. *Global Properties*

The synchrotron emission of the disks and halos of galaxies allows estimates of various quantities which are relevant to the dynamics of the ISM, e.g., the SN rate, ν_{SN}, and the total energy input into the ISM by SNs, $\dot{E}_{SN}^{tot}$. In order to put our investigations into a broader context, we will in the following compare the properties of the five known late-type edge-on spirals which show high-z radio emission above their planes with other galaxies which do not exhibit such emission, or at least to a lesser extent, such as, e.g., NGC 4244, NGC 4565, NGC 5907, and the Milky Way.

The measured quantities upon which we base our computations are collected in Table 3, columns (3)–(6). The r_{SF} was measured from Hα images. The magnetic field strength, B_{min}, was calculated, if no reference is cited, using the standard minimum energy method (see, e.g., Moffet 1975) with a lower and a higher frequency cutoff of 10^7 Hz and 10^{10} Hz, respectively; a nonthermal spectral index of $\alpha_{nth} = -0.7$; and an energy ratio of CR nuclei to electrons of $k = 100$.

With the simplifying assumption that electrons emit all their synchrotron radiation at the maximum frequency ν of the synchrotron spectrum

$$\nu \approx \left(\frac{E}{mc^2}\right)^2 \nu_G \tag{1}$$

(e.g., Longair 1981), with ν_G being the gyrofrequency and m the electron rest mass, the synchrotron emission at a certain frequency ν, $P_{syn}^{tot}(\nu)d\nu$, is related to the total number of CR electrons, $N[E(\nu)]$, emitting at this frequency by

$$P_{syn}^{tot}(\nu)d\nu = N[E(\nu)]\left.\frac{dE}{dt}\right|_{syn}\frac{dE}{d\nu}\,d\nu$$
$$= \nu_{SN}\, q_{SN}\left(\frac{\nu}{\nu_G}\right)^{-x/2}\frac{(mc^2)^2}{x-1}\frac{1}{2\nu_G}\left(1+\frac{U_{rad}}{U_B}\right)^{-1}. \tag{2}$$

Here, we furthermore assume that the timescale for energy losses is much shorter than the timescale for convection/diffusion. x is the spectral index of the CR source spectrum, q_{SN} is the number of electrons produced per SN and per energy interval, and U_{rad} is the energy density of the radiation field below the Klein-Nishima limit. The synchrotron loss rate $dE/dt|_{syn}$ is

$$\left.\frac{dE}{dt}\right|_{syn} = \frac{4}{3}\sigma_T c\left(\frac{E}{mc^2}\right)^2 U_B, \tag{3}$$

with σ_T being the Thompson scattering cross section, U_B the energy density of the magnetic field, and c the speed of light. The power of the synchrotron radiation is thus proportional to the SN rate, ν_{SN}:

$$P_{syn}^{tot}[\mathrm{W\ Hz^{-1}}] = f_{SN} \times \nu_{SN}, \tag{4}$$

where f_{SN} can be estimated from equation (2) and the canonical hydrodynamical energy produced by an SN, $E_{SN} = 10^{51}$ ergs (e.g., Clark & Caswell 1976). About 10% of this energy goes into CR acceleration, and 1% of this fraction (corresponding to $k = 100$, see above) into the acceleration of CR electrons. Therefore, an energy of roughly $E_{SN}^e = 10^{48}$ ergs is available per SN to produce the electron spectrum:

$$E_{SN}^e[\mathrm{ergs}] = q_{SN}\int_{E_{min}}^{\infty} E\left(\frac{E}{mc^2}\right)^{-x} dE$$
$$= -\frac{q_{SN}(mc^2)^2}{2-x}\left(\frac{E_{min}}{mc^2}\right)^{-x+2}. \tag{5}$$

Taking $x = 2.2$ (Völk, Zank, & Zank 1988) and $E_{min} = 1$ GeV, we obtain:

$$q_{SN} = \frac{E_{SN}^e}{(mc^2)^2}\left(\frac{E_{min}}{mc^2}\right)^{x-2}(x-2) = 2.2\times 10^{48}[\mathrm{eV^{-1}}] \tag{6}$$

This result depends only very weakly on the spectral index, x, and the lower cutoff, E_{min}.

We obtain for the proportionality constant f_{SN} [W Hz^{-1} × yr]:

$$f_{SN} = q_{SN}\frac{(mc^2)^2}{x-1}\left(\frac{\nu}{\nu_G}\right)^{-x/2}\frac{1}{2\nu_G}\left(1+\frac{U_{rad}}{U_B}\right)^{-1}$$
$$= \left(\frac{\nu}{1.5\ \mathrm{GHz}}\right)^{-x/2}\left(\frac{B}{5\ \mu\mathrm{G}}\right)^{(x-2)/2}\times 6.4\times 10^{22}, \tag{7}$$

where we have assumed energy equipartition between the mean energy densities of the interstellar radiation field and the magnetic field, $U_{rad} = U_B$. This has been shown to be valid for a large sample of spiral galaxies by Lisenfeld, Völk, & Xu (1995).

The SN rate predicted in this way for our Galaxy (see Table 3) is in reasonable agreement with estimates of other authors

TABLE 3

ENERGY INPUT BY SUPERNOVAE DERIVED FROM RADIO DATA

Object (1)	Morphological Type[a] (2)	D (Mpc) (3)	r_{SF} (kpc) (4)	B_{min} (μG) (5)	$P_{1.49\ GHz}$ (10^{21} W Hz^{-1}) (6)	ν_{SN} (yr^{-1}) (7)	$\dot{E}_A^{tot}$ (10^{-3} ergs s^{-1} cm^{-2}) (8)
NGC 5775	SBc? sp	26.7	9.6	10	18.9	0.28	3.26
NGC 891.....	SA(s)b? sp	9.5	9.6	10[b]	8.2	0.12	1.40
NGC 3044	SB(s)c? sp	20.6	10.0	12.2	6.1	0.09	0.94
NGC 4666	SABc:	14.1	13.0	8.8	9.3	0.14	0.88
NGC 4631	SB(s)d	10.0	17.3	6.5[b]	14.7	0.23	0.83
Milky Way.....	Sbc	...	15	5.0	3.1	0.05	0.23
NGC 5907	SA(s)c: sp	14.9	18.1	5.9	2.6	0.04	0.14
NGC 4565	Sbc	9.7	16.9	6.0	1.5	0.02	0.09
NGC 4244	SA(s)cd? sp	3.1	4.5	<5	0.01	0.002	<0.08

[a] de Vaucouleurs, de Vaucouleurs, & Corwin 1991.
[b] Hummel et al. 1991a.

using different methods. Our result ($\nu_{SN} = 0.05$ yr^{-1}) is the same as the value determined by Tammann (1982) of 0.05 yr^{-1}. It is somewhat higher than the values deduced by van den Bergh (1991) of 0.01–0.022 yr^{-1} and Berkhuijsen (1984) of 0.016–0.022 yr^{-1}. Still, our method gives quite reasonable results, justifying its use to determine ν_{SN} from the measured radio continuum fluxes.

The total energy input into the ISM by SNs is given by

$$\dot{E}_{SN}^{tot} = \nu_{SN} E_{SN} = 3.2 \times 10^{43} \left(\frac{\nu_{SN}}{\mathrm{yr}^{-1}} \right) [\mathrm{ergs\ s}^{-1}] , \qquad (8)$$

where we take, again, $E_{SN} = 10^{51}$ ergs.

For our sample of nine late-type edge-on spirals, we normalized $\dot{E}_{SN}^{tot}$ to the surface area of the actively star-forming disk, $A_{SF} = 2\pi r_{SF}^2$, using the measured radii r_{SF}. The part of the total radio continuum flux coming from the outermost parts of the thin disks extending beyond r_{SF} is negligible for the following calculations, being less than 2%, typically. The mean energy input rates per unit surface area, $\dot{E}_A^{tot} = \dot{E}_{SN}^{tot}/A_{SF}$, are listed in column (8) of Table 3.

A comparison of the $\dot{E}_A^{tot}$ values clearly reveals a systematic trend: the galaxies with the highest mean energy input rates have the most extended and pervasive radio halos. Those with lower $\dot{E}_A^{tot}$ exhibit filamentary radio halo emission (as, e.g., NGC 3044). In NGC 4565 and NGC 5907 marginal evidence of radio halo emission has been found (Hummel, Sancisi, & Ekers 1984). The low-energy end of this distribution is formed by galaxies like, e.g., NGC 4244, with extremely weak radio continuum emission even from their thin disks (Hummel et al. 1984). No outflows or radio continuum from the halo are observed there.

Thus, the scenario describing the dependence of radio halo properties on the SF activity in galaxy disks can be consistently extended to explain observations of other galaxies, including the Milky Way. In fact, the similarity of our observations (see in particular Fig. 3) with the model of the radio emission of the Galaxy by Beuermann, Kanbach, & Berkhuijsen (1985), including detailed features, is striking (their Fig. 9). As in NGC 891 and NGC 4631 (Hummel et al. 1991c), the total radio emission of the Galaxy is also dominated by the halo component, which accounts for about 90% of the total radio power at 408 MHz. Also, exactly as in NGC 891 and NGC 4631, the radial extent of the radio halo is visibly smaller than that of the thin disk, which can be seen clearly by following the slopes of the outer brightness temperature isophotes, e.g., at $T_b = 30$ K.

From this comparison we conclude that the rate at which energy is deposited into the ISM of a galaxy determines whether outflows can occur and that the distribution and surface density of giant H II regions determines the pervasiveness (i.e., the volume filling factor) of the CR plasma and the surface brightness of the radio halo which is eventually created.

There seems to be one slight deviation from the trend outlined in Table 3. NGC 4631 has the largest known radio halo of a normal galaxy, but has a relatively low mean energy input rate compared to NGC 5775 and NGC 891. This deviation is very probably related to the gravitational interaction with its companions, NGC 4627 and NGC 4656. Various H I spurs and bridges are discernible on H I images (Weliachew, Sancisi, & Guélin 1978; Rand 1994), indicating outflows caused by a gravitational drag. Golla & Hummel (1994) and Golla & Wielebinski (1994) argue that the specific way in which the interaction between these three galaxies took place might have been crucial for the present shape and extent of the radio halo of NGC 4631. Gravitationally induced outflows may have produced vertical magnetic fields independent of SF, facilitating the propagation of CRs into the halo.

5.2. *Local Energy Deposition*

The quantities we have introduced up to now describe global parameters of SF activity over the entire disks (and halos) of normal galaxies. However, the lower limit of $\dot{E}_A^{tot}$, which can be gained from such integral properties (see Table 3; ~ 0.1–1×10^{-3} ergs s^{-1} cm^{-2}), does not constrain very precisely the lower threshold enabling outflows.

Local energy inputs can be considerably higher than the average values. In particular the existence of filaments or spurs of radio emission above the most luminous H II regions in external galaxies (§ 3) suggests that the *local* energy input rate into the ISM in such regions, $\dot{E}_A^{tot}$, and its variation across the disk, may determine the conditions for local blowouts and the fine-structure of the disk-halo interface, respectively.

This interpretation is again corroborated by the model for the radio continuum emission of the Milky Way by Beuermann et al. (1985). They found that the halo emission exhibits a dependence on the thin disk's spiral structure. This clearly implies that the halo properties are determined by the local level of SF and thus the energy input into the ISM in the thin disk, and it leads us to the conclusion that the abrupt radial cutoff which we find in NGC 891 and NGC 4631 are most probably located just outside the radii where we view the outermost spiral arms in these systems which have sufficiently high energy input levels per unit surface area, $\dot{E}_A^{tot}$, to enable local blowouts into their halos.

Using as an example an assumed number of 100 giant H II regions above which outflows might occur, each with a diameter of 200 pc (both numbers are typical of late-type spirals; cf. Kennicutt, Edgar, & Hodge 1989), one can calculate that these occupy about 1% of the surface area of the actively star-forming disk of a galaxy like NGC 891, where we measured A_{SF} (above). Accordingly, the local energy input is $\dot{E}_{local}^{tot} \sim 100 \dot{E}_A^{tot} \sim 0.01$–$0.1$ ergs s^{-1} cm^{-2}.

We can at present only conduct orders-of-magnitude calculations because, unfortunately, no sensitive high-resolution (100–200 pc) radio maps of NGC 891 or NGC 4631 are yet available to measure the emissivity of single associations of H II regions above which halo emission is seen. Thus, we cannot yet verify our hypothesis. Hence, high-resolution radio continuum observations of NGC 891 and NGC 4631 are highly desirable.

The local value for $\dot{E}_A^{tot}$ which enables outflows is such an important number because it quantifies the so-called blowout condition, as defined by NI in their chimney model. Precise measurements of this key parameter will enable better model calculations than the orders-of-magnitude estimations which we rely on now. Note that—from a practical point of view—$\dot{E}_A^{tot}$ is a very reliable quantity, because it is independent of the distance of the observed galaxy.

In this study we present only data of late-type spirals (morphological type Sbc or later; Table 3, col. [2]). This is not due to an arbitrary selection: only late-type galaxies host "giant extragalactic H II regions" (GEHRs) (Kennicutt et al. 1989). The correlation between SF activity in the disk and the existence of halo emission indicates that only these are capable of initiating disk-halo interactions. Early-type spirals have

only weak radio continuum disks (e.g., Hummel & Kotanyi 1982). We thus predict that detections of radio halos encompassing nonstarburst galaxies of type Sb or earlier are not to be expected.

5.3. *Energy Densities in the Disks and Halos of NGC 891 and NGC 4631*

Since the SF in the disks of NGC 891 and NGC 4631 is feeding CRs into their halos at rates high enough such that the total radio continuum emission is clearly dominated by the halos (Hummel et al. 1991c), it is suggestive to calculate the energy densities for both galactic components separately and compare them with each other.

In order to derive the total energy of the CR electrons, E_{el}, the radio emission has to be extrapolated over the entire frequency range again, from $\nu_1 = 10$ MHz to $\nu_2 = 10$ GHz. We obtain

$$E_{el}[\mathrm{ergs}] = 1.057 \times 10^{28} \left(\frac{B}{\mu\mathrm{G}}\right)^{-3/2} P_{1.49\ \mathrm{GHz}} \times \left[(\nu_1^{1/2+\alpha_1} - \nu_{\mathrm{break}}^{1/2+\alpha_1}) \left(\frac{-2}{2\alpha_1 + 1}\right) \nu_{\mathrm{break}}^{-\alpha_1} \left(\frac{1.49\ \mathrm{GHz}}{\nu_{\mathrm{break}}}\right)^{-\alpha_2} + (\nu_{\mathrm{break}}^{1/2+\alpha_2} - \nu_2^{1/2+\alpha_2}) \left(\frac{-2}{2\alpha_2 + 1}\right) (1.49\ \mathrm{GHz})^{-\alpha_2} \right] \quad (9)$$

(see, e.g., Moffet 1975). Here, α_1 is the low-frequency nonthermal spectral index, measured for $\nu < \nu_{\mathrm{break}}$, and α_2 is the spectral index for $\nu > \nu_{\mathrm{break}}$, with $\nu_{\mathrm{break}} = 0.8$ GHz. For the calculations we use the $P_{1.49\ \mathrm{GHz}}$ and α_{nth} measurements for the disk and halos of NGC 891 and NGC 4631 by Dahlem (1990), who derived these quantities for both galactic components separately.

Dividing the values calculated in this way by the volume of the star-forming thin disk, V_{SF}, we obtain the mean CR electron energy density, ϵ_{e^-}. Multiplying the resulting value by $k = 100$ (see above), this yields the total CR energy density, ϵ_{CR}:

$$\epsilon_{\mathrm{CR}}^{\mathrm{disk}}[\mathrm{ergs\ cm^{-3}}] = k \frac{E_{\mathrm{el}}^{\mathrm{disk}}}{V_{\mathrm{SF}}} = k \frac{E_{\mathrm{el}}^{\mathrm{disk}}}{\pi r_{\mathrm{SF}}^2 d}. \quad (10)$$

For the volume we use a cylinder with radius r_{SF} and height d. For NGC 891, $d \simeq 400$ pc (Dahlem et al. 1994) and for NGC 4631 we estimate $d = 1.5 \pm 0.5$ kpc, using the maps by Golla & Hummel (1994). The high-resolution map of NGC 891 leads to the most accurate results, because it provides the best constraints on the thickness of the disk of CR electrons.

The same quantity can be calculated for the halos. Here

$$\epsilon_{\mathrm{CR}}^{\mathrm{halo}} = k \frac{E_{\mathrm{el}}^{\mathrm{halo}}}{V_{\mathrm{halo}}} = k \frac{E_{\mathrm{el}}^{\mathrm{halo}}}{\pi r_{\mathrm{halo}}^2 h}, \quad (11)$$

where V_{halo} is the volume of the halo, h is its z-extent (8 kpc for NGC 891 and 20 kpc for NGC 4631; measured from the maps in Figs. 1 and 3), and $r_{\mathrm{halo}} \simeq r_{\mathrm{SF}}$ (§ 2). These are compared to values which we calculate for the Milky Way, adopting the same spectral indices as measured in NGC 891, and taking $h = 9$ kpc and $d = 500$ pc. The numbers listed in Table 4 show that the CR energy densities, ϵ_{CR}, in the disks are considerably (up to one order of magnitude) higher than those in the halos. This means that, although the halos clearly dominate the total radio power, there is still a strong energy density (and thus also CR pressure) gradient, enabling further outflows. Note that ϵ_{CR} depends on the distance to the galaxies, D, so that a direct comparison of values for different galaxies is not as reliable as for E_A^{tot}.

TABLE 4

CR Energy Densities in the Disks and Halos of NGC 891, NGC 4631, and the Milky Way

	α_{nth}				
	$\nu > 0.8$ GHz		$\nu < 0.8$ GHz	ϵ_{CR} (10^{-13} ergs cm^{-3})	
Object	Disk	Halo	Disk = Halo	Disk	Halo
NGC 891	−0.4	−1.1[a]	−0.4	61.6	11.6
NGC 4631	−0.5	−1.1[a]	−0.4	30.1	3.2
Milky Way....	−0.4	−1.1	−0.4	9.6	4.2

[a] Hummel et al. 1991c.

In many previous studies it has been assumed that halos are supported by the entire optically visible disks. We used the sizes of the actively star-forming disks, r_{SF}, to estimate the energy densities in the disks. In comparison with calculations based on the larger disk sizes, the average energy densities derived here are 1.5–2 times higher. Also the CR halos themselves are much smaller than previously thought. This implies that smaller volumes are fed with matter and energy than in the case of purely diffusive CR propagation perpendicular to a plane-parallel magnetic field (in which case ellipsoidal halos, encompassing the entire thin galaxy disks would be seen; see, e.g., Fichtner et al. 1991) and that higher CR energy input rates per unit surface area are available in the disks for the injection of particles and energy into the halos (§ 5.1).

6. COSMIC-RAY DIFFUSION COEFFICIENTS IN THE r- AND z-DIRECTION FOR NGC 891 AND NGC 4631

The differences in the radial extents of the current star-forming disks of NGC 891 and NGC 4631 and those of the synchrotron radiation, Δr (cf. Table 1), provide us with a valuable tool to directly measure the propagation velocity of CR electrons in the outer disks of both galaxies. Since, according to Bicay, Helou, & Condon (1989) this effect is caused by the diffusion of CRs, the diffusion coefficient, $D_r = \Delta r^2 / t_e$ [cm^2 s^{-1}], is a good quantity to measure it. Here t_e denotes the average CR electron lifetime.

Following standard synchrotron theory, the magnetic field strengths in the disks (Table 1, col. [10]) induce synchrotron losses leading to average electron lifetimes of

$$t_e[\mathrm{yr}] \sim 1.06 \times 10^9 \left(\frac{B \sin\theta}{\mu\mathrm{G}}\right)^{-3/2} \left(\frac{\nu}{\mathrm{GHz}}\right)^{-1/2} \quad (12)$$

with $\langle \sin^2 \theta \rangle = \frac{2}{3}$ for isotropically distributed electron velocities (e.g., Condon 1992) and $\nu = 1.49$ GHz for our data. Under the assumption of equipartition of the mean energy densities of the B-field and the interstellar radiation field, $\langle U_B \rangle$ and $\langle U_{\mathrm{rad}} \rangle$ (see § 5.1), synchrotron and inverse Compton losses will be about equally important and thus the average electron lifetime will be half that calculated using equation (12). The relevant values are listed in Table 1, columns (9)–(12).

Since $t_e \propto B^{-3/2}$, the deduction of the magnetic field strength in the galaxy disks leads to one more error source in the calculation of D_r, which adds up on the uncertainty of Δr. We estimate the total uncertainty of D_r to be of the order of ±50%–70%. This estimate does not include possible errors coming from the uncertainty of the distances, D, of the galaxies.

Taking as an example NGC 891, for which we have the best data, D_r is of the order of 1.2×10^{29} cm^2 s^{-1} for $B = 10$ μG.

This implies directly that the CR electrons diffuse so fast that the H II regions will be encompassed by a smoothly distributed population of CRs on timescales of 10^7 yr or less, i.e., still within the typical lifetimes of these regions. This is consistent with the existing radio observations of galaxies.

In taking Δr as the distance which CR electrons propagate away from their places of birth, we assume that there are no (or insignificantly few) H II regions at $r > r_{SF}$. This must be checked very carefully. Unfortunately it cannot be verified based on high-frequency radio observations. Our current low-frequency detection limit in the 1.49 GHz map NGC 891 is about 40 μJy beam^{-1} and the spectral index in the outermost areas of the disk is $\alpha = -1.1$ (Hummel et al. 1991c). An extrapolation to 10.7 GHz shows that one would need a sensitivity of 5 μJy over the same beam area in order to detect the same nonthermal radiation. Thermal emission would be even weaker by almost an order of magnitude (see Klein, Wielebinski, & Beck 1984). Such a sensitivity is far below the limits of current receiver technology.

Nevertheless, the steepness of the spectral index itself in the outermost areas of the disk ($\alpha_{nth} = -1.1$) is very strong evidence for the validity of our assumption. It is much steeper than at $r < r_{SF}$ (where $-0.4 < \alpha_{nth} < -0.85$; Hummel et al. 1991c), indicating strong inverse Compton and synchrotron radiation losses of the CR electrons at $r > r_{SF}$. In the presence of giant H II region complexes, $\alpha_{nth} \sim -0.5$ to -0.7—which is a typical value for SNs and young SNRs—would also be measured at $r > r_{SF}$, in obvious contradiction to our data. In fact, $\alpha_{nth} = -1.1$ at the radial boundaries of the thin disks of both NGC 891 and NGC 4631 is as steep as observed in their halos, at z-distances of $z > 2$ kpc (Hummel et al. 1991c; Hummel & Dettmar 1990). At these heights above the planes we certainly observe an "aged" CR population. Thus, based on spectral index measurements, the population of CR electrons observed in the thin disks of NGC 891 and NGC 4631 at $r > r_{SF}$ must be "old," too, and on-site injection with a spectral index typical of SNRs (~ -0.5) will be negligible.

Similarly, the diffusion coefficient of the CR electrons in the z-direction, $D_z = \Delta z^2/t_e$, can be calculated from the measurements or upper limits on the thickness of the *thin* radio disks. The best results are again available for NGC 891, where a maximum thickness (scale height) of 10″ (460 pc) has been measured (Dahlem et al. 1994). This leads to $D_z \leq 0.2 \times 10^{28}$ cm^2 s^{-1}. For NGC 4631, $d \simeq 1.5$ kpc, which yields $D_z = 1.4 \times 10^{28}$ cm^2 s^{-1}. We emphasize that these numbers are not only meaningful in radial regimes where no halo exists, but also further inward, at $r < r_{SF}$, in those areas between superbubbles—created by multiple SNs in H II regions—where no outflow is currently going on and thus the B-field is plane-parallel. The presence of B-fields in the halos of both NGC 891 and NGC 4631 (Hummel et al. 1988, 1991a) indicates that ordered magnetic fields are torn into the halos. This implies that field lines open into the halos in the outflow regions. Along these lines, the diffusion coefficient for CRs is much higher than D_z. Thus, the abruptness of the radial halo cutoffs is caused by the combination of two effects: expansive/convective blowouts due to high-level SN activity in the disks and, as a consequence of this, faster diffusion of particles in the z-direction.

7. CONCLUSIONS AND FUTURE PERSPECTIVES

We have compiled the currently available observational evidence for a strong dependence of the existence and shapes of radio halos on the level of SF activity in the underlying disks of late-type spirals. While for most of our calculations we use NGC 891 and NGC 4631 as examples (the data for the remaining three galaxies with radio halos are not yet good enough to allow a full analysis), it appears that the dependence of the characteristics of CR radio halos on the disk activity might be a general phenomenon. This is suggested by the fact that our calculations can consistently be extended to other edge-on galaxies with less prominent radio halos or no out-of-the-plane emission, including a very remarkable consistency with the model of the Milky Way's radio halo by Beuermann et al. (1985).

Outflows do not occur everywhere in the disks, but only in those areas where the energy input of SNs and SNRs into the ambient medium is sufficiently high. This leads to a dependence of the halo properties on the underlying spiral arm patterns. We find that the threshold of the energy input rate into the ISM per unit surface area enabling blowouts into the halo is $\dot{E}_A^{tot} > 10^{-4}$ ergs s^{-1} cm^{-2}. The *mean* energy input rate is a good indicator for the occurrence of outflows, whereas the *local* energy input rate by SNs and expanding SNRs controls *where* in the disk of a galaxy individual outflows occur. Here, $\dot{E}_A^{tot} \gtrsim 10^{-2}$ ergs s^{-1} cm^{-2}. Such high levels of energy input are found only in GEHRs in late-type spirals.

Expansion/convection of SN-heated gas appears to play an important role at low z. The spatial distribution of outflows determines the shapes of the radio halos. Galaxies with low energy input rates into their ISM by SNs do not have radio halos. Thus, our measurements corroborate theoretical predictions, e.g., from the "chimney" model of galactic ISM (NI). The abruptness of the radial halo cutoffs is caused by the combined effects of expansion/convection of matter and the break-up of the B-field lines into the halo, and subsequently fast propagation of CRs along the open field lines (Parker 1992).

The reduction of the measured sizes of those parts of the galactic disks feeding the halos (by a factor of up to 2) and of the halos themselves (which have to be fed) by about the same amount infers higher energy densities in the disks than previously estimated and smaller volumes to be fed with matter, meaning that much lower energies are necessary to maintain a galactic radio halo than would be deduced from pure diffusion models.

Based on our data, the diffusion coefficients of CR electrons in galaxy disks have been quantified in two cases. The measured values lie in the range from $D_r = 1.1$–2.5×10^{29} cm^2 s^{-1} (NGC 4631) and $D_r = 1.2 \times 10^{29}$ cm^2 s^{-1} (NGC 891) for radial motions in the disks. In the z-direction within the thin radio disks they are $D_z \leq 0.2 \times 10^{28}$ cm^2 s^{-1} and $D_z = 1.4 \times 10^{28}$ cm^2 s^{-1} for NGC 891 and NGC 4631, respectively.

Further tests await the acquisition of more high-quality data. To this end, we recently obtained a 16 hr integration of NGC 4666 with the VLA at 4.9 GHz. A $\sim 1''$ resolution study of NGC 4631 at 1.5 and 4.9 GHz with full information on the large-scale emission is in preparation. However, it is important that similarly sensitive observations be obtained in different wavebands for all of the very few galaxies with prominent radio halos in order to strengthen our arguments, which could otherwise always be considered as special cases. The data by Irwin (1994) of NGC 5775 should be sensitive enough to render possible the same kind of investigations for that galaxy as done here for NGC 891 and NGC 4631. Two more candidates for such studies are NGC 2820, where Hummel & van der Hulst (1989) found indications of a radio halo, and NGC 2188, in

which Dettmar (1994) detected spectacular Hα filaments emerging from the most luminous H II regions in the disk.

It is a pleasure to thank E. Brinks for numerous valuable comments.

We cordially thank M. Dumke, M. Lehnert, W. van Driel, and R. Walterbos for providing us with results and data prior to publication. H.-J. Völk, T. M. Heckman, J. M. van der Hulst, J. A. Irwin, and A. Ferguson are thanked for very useful suggestions/information. We thank the referee, E. Hummel, for many useful comments. Thanks are also due to S. M. Baggett for improvements to the manuscript. U. L. is supported by Deutsche Forschungsgemeinschaft (DFG) with a Postdoctoral Fellowship. G. G. is supported by von Humboldt Stiftung with a Postdoctoral Fellowship. M. D. is partly supported by NASA under grant NAGW-4025.

REFERENCES

Allen, R. J., Baldwin, J. E., & Sancisi, R. 1978, A&A, 62, 397
Berkhuijsen, E. M. 1984, A&A, 140, 431
Beuermann, K., Kanbach, G., & Berkhuijsen, E. M. 1985, A&A, 153, 17
Bicay, M. D., Helou, G., & Condon, J. J. 1989, ApJ, 338, L53
Bregman, J. N., & Pildis, R. A. 1994, ApJ, 420, 570
Breitschwerdt, D., McKenzie, J. F., & Völk, H. J. 1991, A&A, 245, 79
———. 1993, A&A, 269, 54
Clark, D. J., & Caswell, J. L. 1976, MNRAS, 174, 267
Condon, J. J. 1992, ARA&A, 30, 575
Dahlem, M. 1990, dissertation thesis, Univ. of Bonn
Dahlem, M., Dettmar, R.-J., & Hummel, E. 1994, A&A, 290, 384
Dettmar, R.-J. 1990, A&A, 232, L14
———. 1992, Fund. Cosmic Phys., 15, 145
———. 1994, in The Physics of the Interstellar Medium and Intergalactic Medium, ed. A. Ferrara, C. Heiles, C. McKee, & P. Shapiro (ASP Conf. Ser.), in press
Dettmar, R.-J., & Golla, G. 1995, in preparation
de Vaucouleurs, G., de Vaucouleurs, A., Corwin, H. G., Buta, R. J., Paturel, G., & Fouqué, P. 1991, Third Reference Catalogue of Bright Galaxies (New York: Springer)
Duric, N., & Bloemen, H. 1989, in Proc. 21st Internat. Cosmic Ray Conf. (Sydney), Session OG, 217
Ekers, R. D., & Sancisi, R. 1977, A&A, 54, 973
Fichtner, H., Neutsch, W., Fahr, H. J., & Schlickeiser, R. 1991, ApJ, 371, 98
Field, G. B., Goldsmith, D. W., & Habing, H. J. 1969, ApJ, 155, L49
García-Burillo, S., Guélin, M., Cernicharo, J. J., & Dahlem, M. 1992, A&A, 266, 21
Golla, G. 1993, dissertation thesis, Univ. of Bonn
Golla, G., & Hummel, E. 1994, A&A, 284, 777
Golla, G., & Wielebinski, R. 1994, A&A, 286, 733
Habe, A., & Ikeuchi, S. 1980, Prog. Theor. Phys., 64, 1995
Hummel, E., Beck, R., & Dahlem, M. 1991a, A&A, 248, 23
Hummel, E., Beck, R., & Dettmar, R.-J. 1991b, A&AS, 87, 309
Hummel, E., Dahlem, M., van der Hulst, J. M., & Sukumar, S. 1991c, A&A, 246, 10
Hummel, E., & Dettmar, R.-J. 1990, A&A, 236, 23
Hummel, E., & Kotanyi, C. G. 1982, A&A, 106, 183
Hummel, E., Lesch, H., Wielebinski, R., & Schlickeiser, R. 1988, A&A, 197, L29
Hummel, E., Sancisi, R., & Ekers, R. D. 1984, A&A, 133, 1
Hummel, E., & van der Hulst, J. M. 1989, A&AS, 81, 51
Ikeuchi, S. 1988, Fund. Cosmic Phys., 12, 255
Irwin, J. A. 1994, ApJ, 429, 618
Kennicutt, R. C., Edgar, B. K., & Hodge, P. W. 1989, ApJ, 337, 761
Klein, U., Wielebinski, R., & Beck, R. 1984, A&A, 135, 213
Lehnert, M. D. 1992, Ph.D. thesis, The Johns Hopkins Univ.
Lehnert, M. D., & Heckman, T. M. 1995, ApJS, 97, 89
Lisenfeld, U., Völk, H. J., & Xu, C. 1995, A&A, submitted
Longair, M. S. 1981, High Energy Astrophysics (Cambridge: Cambridge Univ. Press)
McKee, C. F., & Ostriker, J. P. 1977, ApJ, 218, 148
Moffet, A. T. 1975, in Stars and Stellar Systems, 9, Galaxies and the Universe, ed. A. Sandage, M. Sandage, & J. Kristian (Chicago: Univ. of Chicago Press), 211
Norman, C. A., & Ikeuchi, S. 1989, ApJ, 345, 372 (NI)
Parker, E. N. 1992, ApJ, 401, 137
Rand, R. J. 1994, A&A, 285, 833
Rand, R. J., Kulkarni, S. R., & Hester, J. J. 1990, ApJ, 352, L1
———. 1992, ApJ, 396, 97
Shapiro, P. A., & Field G. B. 1976, ApJ, 205, 762
Siemieniec, G., & Cesarsky, C. 1991, A&A, 245, 418
Sukumar, S., Velusamy, T., & Klein, U. 1988, MNRAS, 231, 765
Tammann, G. A. 1982, in Supernovae: A Survey of Current Research, ed. M. J. Rees & R. J. Stoneham (Dordrecht: Reidel), 371
Tomisaka, K., Habe, A., & Ikeuchi, S. 1981, Ap&SS, 78, 273
Tully, R. B. 1988, Nearby Galaxies Catalog (Cambridge: Cambridge Univ. Press)
van den Bergh, S. 1991, Phys. Rep., 204 (6), 385
van Driel, W., de Graauw, Th., de Jong, T., & Wesselius, P. R. 1993, A&AS, 101, 207
Völk, H. J., Zank, L. A., & Zank, G. P. 1988, A&A, 198, 274
Wang, Q., Walterbos, R. A. M., Steakley, M. F., Norman, C. A., & Braun, R. 1995, ApJ, 439, 176
Weliachew, L., Sancisi, R., & Guélin, M. 1978, A&A, 65, 37